

# The impact of niobium doping upon the magnetotransport properties of the oxygen-deficient perovskite $\text{SrCo}_{1-x}\text{Nb}_x\text{O}_{3-\delta}$

T. Motohashi,\* V. Caignaert, V. Pralong, M. Hervieu, A. Maignan, and B. Raveau  
Laboratoire CRISMAT, UMR CNRS ENSICAEN 6508, 6 bd Maréchal Juin  
14050 CAEN Cedex 4 France

The oxygen-deficient perovskite cobaltite  $\text{SrCo}_{1-x}\text{Nb}_x\text{O}_{3-\delta}$  was synthesized by direct solid-state reaction and its magnetotransport properties were investigated. This cobaltite exhibits an unusual ferromagnetic behavior with a transition temperature  $T_m = 130\text{-}150$  K and a spin glass like behavior below  $T_m$ . Importantly, this phase reaches a large magnetoresistance (MR) value,  $\text{MR} \equiv -(\rho_H - \rho_0) / \rho_0 = 30\%$  at 5 K in 7 T. The large MR effect is believed to be related to the disordered magnetic state induced by the Nb-for-Co substitution.

\* Corresponding author

Permanent address: Materials and Structures Laboratory, Tokyo Institute of Technology, 4259 Nagatsuta, Midori-ku, Yokohama 226-8503, Japan.

E-mail: t-mot@msl.titech.ac.jp

Phone: +81-45-924-5318

Fax: +81-45-924-5339

One of the most attractive phenomena in functional transition-metal oxides deals with their large magnetoresistance (MR) properties. The first example is the colossal MR effect in perovskite manganites, for which the MR magnitude, defined as  $MR \equiv -(\rho_H - \rho_0) / \rho_0$ , often surpasses 90% (for a review see Ref. 1). Besides, cobaltites with the perovskite structure were also found to exhibit large MR values, as illustrated for  $\text{La}_{1-x}\text{Sr}_x\text{CoO}_3$  [2-4] and the ordered oxygen-deficient perovskite  $\text{LnBaCo}_2\text{O}_{5.4}$  [5], whose MR ranges from 12.5% to 50% in 7 T at low temperatures.

In contrast to perovskite manganites, the magnetotransport properties of cobaltite perovskites do not seem to cover a broad range of composition. For instance, no MR effect has been reported to date about the stoichiometric  $\text{SrCoO}_3$  synthesized using electrochemical oxidation [6] or high pressure technique [7] and the MR effect was found to be negligible in the oxygen-deficient perovskite  $\text{SrCoO}_{2.75}$ , prepared by a two-step method [8]. However, a MR value of 12% in 7 T at 5 K was recently reported for the Sc-substituted oxygen-deficient perovskite  $\text{SrCo}_{1-x}\text{Sc}_x\text{O}_{3-\delta}$  [9]. This suggests that the introduction of a  $d^0$  cation, like  $\text{Sc}^{3+}$ , on the cobalt sites, not only stabilizes the perovskite structure but also is susceptible to induce large MR. We have thus explored the possibility to stabilize the cobalt perovskite by a  $d^0$  cation with a higher valency such as  $\text{Nb}^{5+}$ . In this letter, we report on the magnetotransport properties of the oxygen-deficient perovskites  $\text{SrCo}_{1-x}\text{Nb}_x\text{O}_{3-\delta}$ . We show that the latter exhibits resistivity, one order of magnitude smaller than for the Sc-substituted cobaltite and a MR value three times higher. We also suggested that this high MR value is closely related to the presence of a disordered magnetic state induced by the Nb-for-Co substitution.

Samples of  $\text{SrCo}_{1-x}\text{Nb}_x\text{O}_{3-\delta}$  with  $x = 0.05, 0.10, 0.15,$  and  $0.20$  were prepared from powder mixtures of  $\text{SrCO}_3$ ,  $\text{Co}_3\text{O}_4$ , and  $\text{Nb}_2\text{O}_5$  with appropriate ratios which were calcined in flowing  $\text{O}_2$  at  $800^\circ\text{C}$  for 12 h. This calcined powder was ground, pelletized, and fired in flowing  $\text{O}_2$  at  $1200^\circ\text{C}$  for 12 h, followed by slow cooling down to room temperature. A part of the samples was subsequently post-annealed at  $500^\circ\text{C}$  for 24 h in high-pressure oxygen (10 MPa). X-ray powder diffraction (XRPD) analysis (detailed elsewhere [10]) indicated that all the samples were single phase with the perovskite structure, except for the post-annealed  $x = 0.05$  sample which was partially decomposed after annealing, leading to the formation of  $\text{Sr}_6\text{Co}_5\text{O}_{15}$  as an impurity. The lattice parameter of the cubic subcell was found to linearly increase with  $x$  from  $3.8560 \text{ \AA}$  for  $x = 0.05$  to  $3.8797 \text{ \AA}$  for  $x = 0.20$  in the as-synthesized samples and from  $3.8648 \text{ \AA}$  for  $x = 0.10$  to  $3.8776 \text{ \AA}$  for  $x = 0.20$  in the  $\text{O}_2$ -annealed samples.

The electron diffraction (ED) analysis confirmed a good crystallinity of the compounds. The ED patterns exhibit a set of intense reflections characteristic of a perovskite-related structure, the presence of weaker extra spots suggesting additional ordering phenomena which will be reported elsewhere. The energy dispersive analysis (EDS) performed with a kevox analyzer mounted on a transmission electron microscope, JEOL 200 CX, confirmed the nominal cationic compositions and the homogeneity of the samples. The chemical analysis using redox titration leads to oxygen contents ranging from  $\text{O}_{2.74}$  ( $x = 0.05$ , as-synthesized) to  $\text{O}_{2.83}$  ( $x = 0.20$ ,  $\text{O}_2$ -annealed). It was shown that the cobalt valency decreases from  $+3.39$  for  $x = 0.05$  to  $+3.30$  for  $x = 0.20$  in the as-synthesized samples and slightly increases by  $\text{O}_2$ -annealing, e.g.  $+3.33$  for  $x = 0.20$  [10].

The temperature dependence of resistivity  $\rho$  (Fig. 1), measured using a four-point-probe apparatus (PPMS; Quantum Design) shows a similar behavior, to that observed for  $\text{SrCo}_{1-x}\text{Sc}_x\text{O}_{3-\delta}$  [9], i.e.  $\rho$  increases systematically with the Nb content  $x$ , due to the decrease in the number of conducting paths, interrupted by  $\text{Nb}^{5+}$  species. In both cases,  $\rho$  decreases by  $\text{O}_2$  annealing, in agreement with the increase in  $\text{Co}^{4+}$  content. Nevertheless, it must be emphasized that for low  $x$  values ( $x \leq 0.10$ ) the resistivity of the Nb-samples at low  $T$  is an order of magnitude smaller than that of the Sc-phase.

Magnetic properties were investigated using a vibrating sample magnetometer and a dc-ac SQUID magnetometer. The dc magnetization ( $M$ ) curves show a significant increase of  $M$  at low  $T$  (Fig. 2), indicating the presence of ferromagnetic interactions. The magnetic transition temperature  $T_m = 130\text{-}150$  K, determined by means of ac-susceptibility measurements (a representative result is presented in Fig. 3), does not strongly depend on the Nb content ( $x$ ) while it slightly increases by  $\text{O}_2$  annealing. The absolute value of  $M$  rapidly decreases with increasing  $x$ , being consistent with the fact that non-magnetic  $\text{Nb}^{5+}$  cations dilute the magnetic interaction. The magnetic behavior gets enhanced by  $\text{O}_2$  annealing for all the  $x$  values, due to the increase in the concentration of magnetic  $\text{Co}^{4+}$  species.

These magnetic data show that  $\text{SrCo}_{1-x}\text{Nb}_x\text{O}_{3-\delta}$  is, like the Sc-substituted cobaltites, clearly different from a typical ferromagnet. Its  $M$  value at 5 K is not indeed saturated in 5 T, with a value of  $\sim 0.8 \mu_B/\text{Co}$ , i.e. much smaller than that reported for  $\text{SrCoO}_3$ , 1.8-2.1  $\mu_B/\text{Co}$  [6,7]. Nevertheless, it is worth pointing out that this value is higher than for the

Sc-phase,  $0.3 \mu_B/\text{Co}$  [9]. In fact the magnetic susceptibility in the field-cooled process (inset of Fig. 2) and the frequency dependent ac-susceptibility peak (Fig. 3), clearly indicate a disordered magnetic state, characteristic of a spin glass or a cluster glass.

The  $\rho(T)$  curves in 7 T (Fig. 1) show large MR effects. The MR vs  $H$  measurements were performed at several temperatures. A typical result is shown in Fig. 4. The MR value monotonically increases with decreasing temperature. A large hysteresis is seen only at 5 K for all the samples. The MR effect closely correlates with the  $M(H)$  curve (inset of Fig. 4): the resistivity is highest at the coercive field,  $\approx 0.6$  T, suggesting a maximum number of magnetic domain boundaries as shown for a  $\text{Sr}_2\text{CoO}_4$  thin film [11]. The MR values (in 7 T) at 5, 50, 100, and 150 K were plotted in Fig. 5 against the Nb content,  $x$ . The MR value in 7 T is as large as 30% at 5 K and still 27% even at 50 K for the  $x = 0.15$  and 0.20  $\text{O}_2$ -annealed samples. This value is three times larger than that reported for  $\text{SrCo}_{1-x}\text{Sc}_x\text{O}_{3-\delta}$  [9].

The monotonic increase in MR below  $T_m$  implies that the negative MR effect mainly stems from spin-dependent scattering of carriers which is related to the ferromagnetic state. The correlation between  $\text{MR}(H)$  and  $M(H)$  also supports this hypothesis. Moreover, for  $x = 0.2$  the magnetization is significantly enhanced by  $\text{O}_2$  annealing, and accordingly, the MR magnitude increases (Figs. 2 and 5). Thus, it is obvious that there exists a threshold in the ferromagnetic interaction for the appearance of a large MR effect. However, ferromagnetism is not the only factor required for large MR as shown by comparing with the  $\text{SrFe}_{1-x}\text{Co}_x\text{O}_{3-\delta}$  series [8] which exhibits smaller MR effect ( $\sim 12\%$ ) in spite of large magnetic moment ( $> 1 \mu_B/\text{f.u.}$ ). More probably, the magnetic

disorder induced by Nb-for-Co substitution, leading to a spin glass behavior, renders an additional contribution in the enhanced MR: i.e. the field-induced ferromagnetism further reduces spin-dependent scattering of carriers. The comparison of the  $x = 0.10$  as-synthesized and  $x = 0.15$  annealed samples (or the 0.15 as-synthesized and 0.20 annealed samples), which both have almost the same  $\rho$  and  $M$  values, but exhibit different MR values of 26% and 30% (24% and 31%) at 5 K, respectively, is in agreement with this view point.

Finally, it must be emphasized that this Sr-rich series  $\text{SrCo}_{1-x}\text{Nb}_x\text{O}_{3-\delta}$  and La-rich series  $\text{La}_{1-x}\text{Sr}_x\text{CoO}_3$  exhibit very different magnetic and MR properties. For instance,  $\text{La}_{0.7}\text{Sr}_{0.3}\text{CoO}_3$  is a ferromagnetic metal (Curie temperature  $T_C = 220\text{-}240$  K) with only small MR values ( $\approx 9\%$  in 6 T) [3,4] whereas  $\text{SrCo}_{0.8}\text{Nb}_{0.2}\text{O}_{2.83}$  has a disordered magnetic state with much larger MR, in spite of the same cobalt valency of these two oxides ( $= +3.3$ ). Clearly, both magnetic dilution through Nb-for-Co substitution and oxygen vacancies are important ingredients to induce large MR in the perovskite cobaltites.

In summary, we have shown the possibility to synthesize Nb-substituted oxygen-deficient perovskites  $\text{SrCo}_{1-x}\text{Nb}_x\text{O}_{3-\delta}$ , with large negative MR, reaching 30% at 5 K in 7 T. The excellent MR property of this unusual weak ferromagnet with  $T_m = 130\text{-}150$  K may originate from the existence of the disordered magnetic state, induced by Nb-for-Co substitution. Detailed investigations of magnetism and structure of the present compound will be necessary to further understand these phenomena.

## References

1. C.N.R. Rao, and B. Raveau (Eds.), Colossal Magnetoresistance Oxides, Charge Ordering and Related Properties of Manganese Oxides, World Scientific, Singapore, 1998; Y. Tokura (Ed.), Colossal Magnetoresistance Oxides, Gordon & Breach, London, 1999.
2. G. Briceno, H. Chang, X. Sun, P.G. Schultz, X.D. Xiang, Science **270**, 273 (1995).
3. S. Yamaguchi, H. Taniguchi, H. Takagi, T. Arima, and Y. Tokura, J. Phys. Soc. Jpn. **64**, 1885 (1996).
4. R. Mahendiran and A.K. Raychaudhuri, Phys. Rev. B **54**, 16044 (1996).
5. C. Martin, A. Maignan, D. Pelloquin, N. Nguyen, and B. Raveau, Appl. Phys. Lett. **71**, 1421 (1997).
6. P. Bezdzicka, A. Wattiaux, J.C. Grenier, M. Pouchard, and P. Hagenmuller, Z. anorg. Allg. Chem. **619**, 7 (1993).
7. S. Kawasaki, M. Takano, and Y. Takeda, J. Solid State Chem. **121**, 174 (1996).
8. A. Maignan, C. Martin, N. Nguyen, and B. Raveau, Solid State Sciences **3**, 57 (2001).
9. A. Maignan, D. Pelloquin, D. Flahaut, and V. Caignaert, J. Solid State Chem. **177**, 3693 (2004).
10. T. Motohashi, V. Caignaert, V. Pralong, M. Hervieu, A. Maignan, and B. Raveau, Phys. Rev. B (2005) in press.
11. J. Matsuno, Y. Okimoto, Z. Fang, X.Z. Yu, Y. Matsui, N. Nagaosa, M. Kawasaki, and Y. Tokura, Phys. Rev. Lett. **93**, 167202 (2004).

## Figure captions

Fig. 1:

Temperature dependence of resistivity ( $\rho$ ) for the as-synthesized (a) and O<sub>2</sub>-annealed (b) SrCo<sub>1-x</sub>Nb<sub>x</sub>O<sub>3- $\delta$</sub>  samples. The solid and broken curves show  $\rho$  data recorded in 0 T and 7 T, respectively.

Fig. 2:

Temperature dependence of magnetization ( $M$ ) for the SrCo<sub>1-x</sub>Nb<sub>x</sub>O<sub>3- $\delta$</sub>  samples. The data were recorded in the zero-field-cooling mode (0.25 T) using a vibrating sample magnetometer. The inset shows susceptibility data for the  $x = 0.10$  O<sub>2</sub>-annealed sample. The data were recorded in 0.3 T using a SQUID magnetometer.

Fig. 3:

Temperature dependence of ac-susceptibility, (a)  $\chi'$  and (b)  $\chi''$ , for the O<sub>2</sub>-annealed  $x = 0.10$  sample. The data were recorded in an ac-field of 3 Oe with frequencies of 1, 10, and 100 Hz. The transition temperature  $T_m$  is marked with an arrow.

Fig. 4:

MR vs  $H$  plots for the  $x = 0.15$  O<sub>2</sub>-annealed sample at 5, 50, 100, 150, and 200 K. In each measurement, the sample was zero-field-cooled, and the magnetic field was swept from 0 to 7 T, then 7 to -7 T. A large hysteresis is seen only at 5 K. The inset shows the  $M$  vs  $H$  loop at 5 K for the same sample.

Fig. 5:

The MR values (in 7 T) at 5, 50, 100, and 150 K against the Nb content,  $x$ . The MR values were obtained from the MR vs  $H$  measurements. Open and closed symbols denote the as-synthesized and O<sub>2</sub>-annealed samples, respectively.

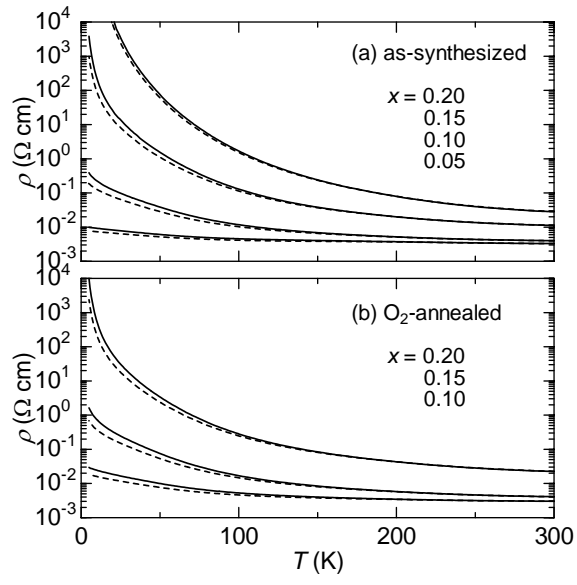


Fig. 1: Motohashi *et al.*

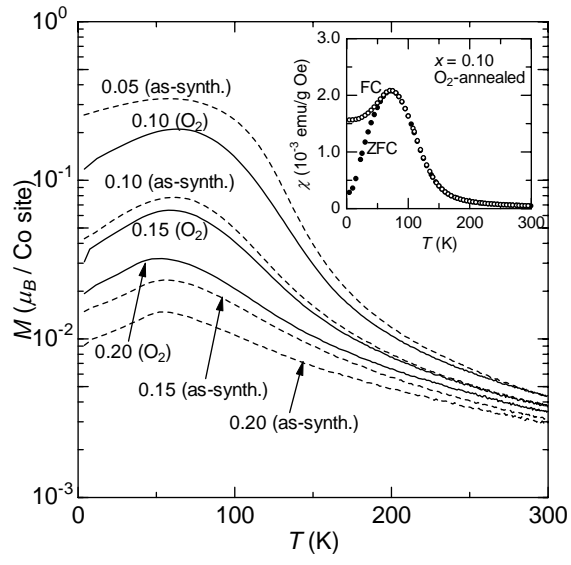


Fig. 2: Motohashi *et al.*

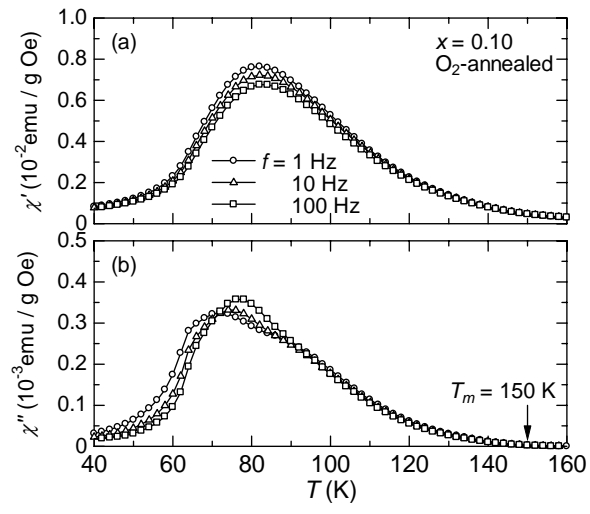


Fig. 3: Motohashi *et al.*

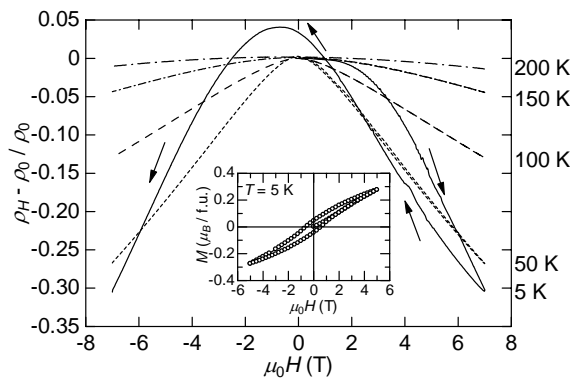


Fig. 4: Motohashi *et al.*

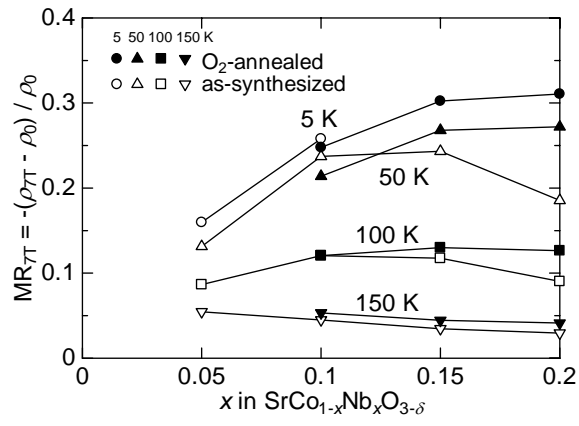


Fig. 5: Motohashi *et al.*